

Sensing and Force-Feedback Exoskeleton (SAFE) Robotic Glove

Pinhas Ben-Tzvi, *Senior Member, IEEE*, and Zhou Ma, *Student Member, IEEE*

Abstract—This paper presents the design, implementation and experimental validation of a novel robotic haptic exoskeleton device to measure the user's hand motion and assist hand motion while remaining portable and lightweight. The device consists of a five-finger mechanism actuated with miniature DC motors through antagonistically routed cables at each finger, which act as both active and passive force actuators. The SAFE Glove is a wireless and self-contained mechatronic system that mounts over the dorsum of a bare hand and provides haptic force feedback to each finger. The glove is adaptable to a wide variety of finger sizes without constraining the range of motion. This makes it possible to accurately and comfortably track the complex motion of the finger and thumb joints associated with common movements of hand functions, including grip and release patterns. The glove can be wirelessly linked to a computer for displaying and recording the hand status through 3D Graphical User Interface (GUI) in real-time. The experimental results demonstrate that the SAFE Glove is capable of reliably modeling hand kinematics, measuring finger motion and assisting hand grasping motion. Simulation and experimental results show the potential of the proposed system in rehabilitation therapy and virtual reality applications.

Index Terms—Data gloves, force measurement, grasping, haptic interfaces.

I. INTRODUCTION

THE HUMAN hand is capable of obtaining information as well as executing complex tasks. The hand has a variety of functions, though the most important are the sensory and the motor functions [1], [2]. According to topography, sensibilities are classified into two categories: 1) superficial sensation that provides skeleton and muscles position information, and 2) deep sensation that provides external stimuli. It is the association of both the sensory function and the motor function that makes the hand an important organ that provides information and accomplishes daily tasks. As a wearable device on a human hand, in order to better interact with the hand or provide rehabilitation function to the fingers, the haptic glove should have similar functions to the human hand, including the ability to measure finger position and force, and provide active force feedback to the hand. With all these previously mentioned functions, haptic

gloves would better assist the creation of virtual objects in virtual reality (VR) [3]–[5], enhance the remote control of teleoperation [6]–[8] and provide active movement assistance for rehabilitation [9]–[11].

A. Finger Joint Angles Measurement Methods

With the technological developments in recent years, the most common instruments and methods used for measuring hand kinematics include glove-based electro-mechanical sensing devices [12]–[14] and marker-based hand motion tracking with [15]–[17] or without the use of markers [18]–[21].

Most of those data gloves were constructed from plastic or Lycra to allow flexible movement, with a variety of sensors to measure the angle of the bend, such as resistive ink sensors, flexible tubes, strain gauges and optical fibers [12]. The gloves were both inexpensive and lightweight but not particularly accurate, since the crude gesture recognition abilities were sufficient for the specific application for which they were designed for (e.g., gaming). Markerless visual tracking systems have the potential to provide natural, noncontact methods to measure hand motions. However, since the hand contains 27 degrees of freedom [22], such high-dimensional state-space usually demands intensive computation, which leads to a low update rate. Marker-based capture systems usually consist of surface markers and image sensors (e.g., the Vicon motion systems). They offer higher precision and faster measurements compared with the markerless vision-based hand sensing system. However, they are inconvenient to use since a number of the markers need to adhere to the hands during the entire measurement procedure and require time-consuming calibration.

B. Force Measurement Methods

From literature, we can find that there are mainly three approaches to measure the contact force between the human fingertip and an object:

The first approach is to attach a force sensor such as a strain gauge to the object. This method permits precise measurement with high resolution sensor, but the disadvantage is that users have to develop different kinds of custom-made devices for different experiments. To measure three different objects, three sets of force sensors need to be attached and three calibration procedures need to be performed. As more objects are added in this experiment, the method becomes increasingly tedious.

The second method is to insert a thin force sensing resistor (FSR, InterLink Electronics Inc.) between the fingertip and the object. The main advantages of these sensors are their low cost, small thickness and flexibility, which allows the sensors to

Manuscript received June 25, 2014; revised October 17, 2014; accepted November 09, 2014. Date of publication December 04, 2014; date of current version November 04, 2015.

The authors are with the Robotics and Mechatronics Lab, George Washington University, Washington, DC, 20052 USA (e-mail: bentzvi@gwu.edu; mazhou@gwu.edu).

Color versions of one or more of the figures in this paper are available online at <http://ieeexplore.ieee.org>.

Digital Object Identifier 10.1109/TNSRE.2014.2378171

easily fit in a data glove. This method applies to various types of experiments [23], [24]. The main drawback of this method is that the user cannot feel the tactile information from the object since the sensor is between the fingertip and the object. As a result, the sense of touch of that finger is deadened [25] and the sensor may modify the user's behavior (grasp force). Besides, the nonlinearity, drift, saturation and hysteresis of the FSR make them difficult to be applied in custom-fabricated solutions [26].

Mascaro *et al.* proposed a camera based on the method to detect contact forces by analyzing the color change of a fingernail [27]–[29] such that different color changes correspond to different contact forces. This method allows the finger to directly contact the object without obstructing the natural haptic sense of the finger. However, the disadvantages of this method are obvious; the result varies significantly from person to person, and the calibration procedure is difficult.

Recently, some researches have proposed a new way to measure the force between the finger and the object during grasping [30]. The idea involves measuring the deformation of the finger pad when it's contacting the object. When the finger touches the object, normal deformation of the finger pad changes the width of the finger. This change can be measured by the sensor at the side of the fingertip, thus the user can touch the object without putting any sensors between the finger and the object. This method overcomes the disadvantages mentioned above and was adopted into the SAFE glove design.

C. Force Feedback Gloves

Haptic gloves equipped with actuators can provide active force-feedback to the hand of the user. Force information is critical since without force feedback it is difficult to understand whether an object is in a stable grasp position for the operator in Virtual Reality (VR) and teleoperation applications. Recently, several five-finger force feedback devices have been developed [10], [31]–[36]. Those finger haptic devices can be divided into passive or active force feedback devices.

The passive haptic gloves [3], [34], [37] use brake, controllable dampener or electromagnetic clutch to provide the resistance force. The user can feel the resistance force when the passive actuator is engaged. Torque can easily be controlled by the passive force haptic devices since the torque is proportional to the current, or the magnetic field, which excites the coil or the damper. The passive devices never harm the user, even if the devices become uncontrollable. Therefore, safety is another advantage of these haptic gloves. However, passive devices still have problems compared to active force feedback devices: (1) the passive actuators are heavy and bulky, (2) due to the inductance elements, they take a relatively long time to respond, which means that they may not be suitable for real-time control, (3) when the hand remains motionless, they cannot provide any force feedback.

The active force feedback gloves primarily use a bilateral force output method. Motor or pneumatic cylinders are controlled to provide the force feedback. One potential problem is that the device may hurt the user's finger if it becomes uncontrollable. To avoid this failure, most of the active haptic gloves limit the maximum output force to about 10 N.

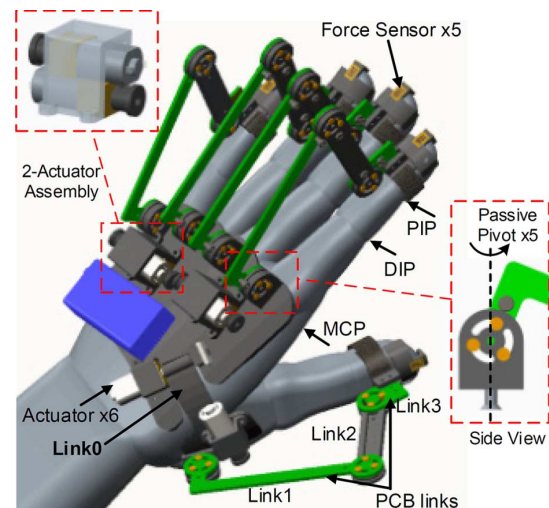


Fig. 1. CAD model of the Hand and SAFE glove system.

D. The State-of-the-Art

The RMII-ND [5], [38] is the most cited noncommercial haptic glove. By actuating a pneumatic piston located inside the palm, the glove can generate a force of up to 16 N to each finger (without the little finger), which opposes the closing of the hand (single direction force). With a weight of only 100 g, the glove is lightweight and comfortable to wear. Each piston has sensors to measure its displacement and the finger position. Air compressor and other supporting devices are required to power and control the RMII-ND. However, the RMII-ND may be limited in its applications to laboratory and clinical settings. This is due to its limited workspace, heavy weight of the air compressor and potential difficulty for patients who are affected with spasticity and their ability to put on the glove.

The CyberGrasp [39] is one of the most successful haptic gloves available on the market. The glove is mounted on the back of the hand and weighs 350 g. The actuation tendons pull the glove mechanism to provide force feedback up to 12 N to each finger in the direction of oppose the fingers closing (only one direction force feedback). The separate control and actuator unit has a weight of 20 kg, which makes the device's portability difficult. Due to lack of position sensors, the CyberGrasp needs an extra data glove (CyberGlove) to provide sensing. Though it costs over \$100K, the Cybergrasp is one of the most typically cited commercially available systems. Therefore, the CyberGraps could be expensive, fatiguing to the operators, unreliable and intrusive [40].

Numerous research efforts have attempted to recreate hand forces, but in general they don't have all the three functions that were mentioned above. If we can measure and record (position, rotation and force) how humans grasp objects effectively, this will greatly help to program a robotic hand for various grasping functions. The authors believe that, for the haptic glove, it is fundamental to be able to measure the hand position and contact forces quantitatively to provide force feedback for various applications, such as VR, rehabilitation and teleoperation. Thus, greater detail is required for improving the five-finger haptic glove design. The authors then propose using a novel haptic-glove (CAD model is shown in Fig. 1) based on an

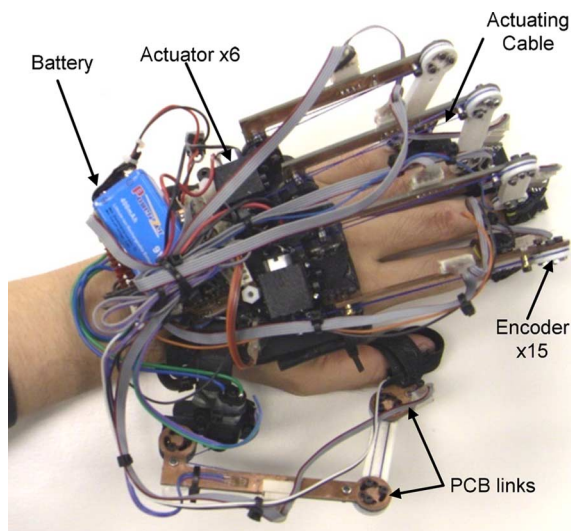


Fig. 2. SAFE Glove prototype worn on a hand.

articulated hand model to measure finger length from multiple movements. This device is a newly developed, lightweight and portable haptic glove that fits on a bare hand. It is adaptable to a wide variety of finger sizes without constraining the range of motion. This makes it possible to accurately and comfortably track the complex motion of the finger joints and add a sense of touch to the users' fingers. Based on this glove, a novel method was developed to generate a hand kinematic model, which includes the length of finger phalanges and joints locations.

This paper is organized as follows. Section II briefly summarizes the mechanical and electrical design of the glove system. Section III discusses a method for measuring finger length by modelling the hand using least squares circle fitting procedure from a collection of points, and uses the proposed glove to realize the method. Section IV describes a hand motion experiment to evaluate both the glove design and the hand model. Finally, Section V provides the conclusions and discusses future work.

II. FIVE-FINGERED HAPTIC GLOVE DESIGN

A. Mechanical Design

The five-fingered haptic glove is a follow-up to the two-finger glove developed [41]. It is a lightweight, portable, sensing/actuating system that fits on a bare hand and is attached to the finger tips as shown in Fig. 2. The total weight of the five-fingered prototype is 275 g, including one 9 V rechargeable battery (20 g), one control unit (25 g), six actuator assemblies (30 g each) and mechanical exoskeleton (50 g).

The links of the five-fingered glove form a series of three linkages over each individual finger [41]. According to [42] the human fingers axes are not orthonormal to the sagittal plane. Human fingers do not bend in a single plane since the relative orientations of the finger joint axes are not perfectly parallel to each other. A simple planar linkage was not acceptable because the joint-axes misalignment between the finger and the glove mechanism can generate uncomfortable translational forces on

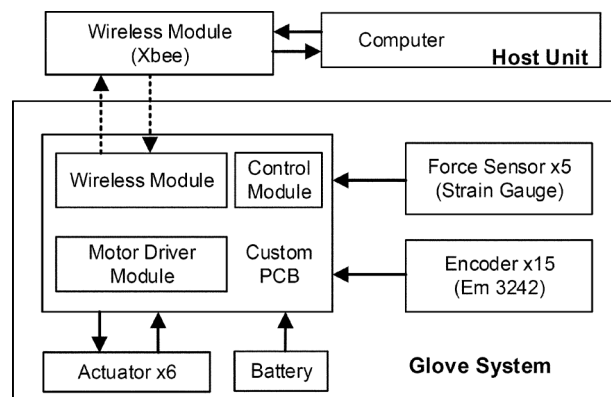


Fig. 3. Electrical design diagram of the SAFE Glove system.

user fingers. As a result, the mechanism limits the range of motion of the finger and the measurement accuracy [43]. The two features of the SAFE Glove, which eliminate the joint axes misalignment problem, are the passive pivot and flexible link of the printed circuit board (PCB). The passive pivot joint allows the finger to bend in the direction of abduction/adduction freely, while minimizing the undesired forces on the articulations and maintaining the accuracy of the sensor measurement. This allows a long PCB link to bend as the finger bends to compensate for the joint inclination, while keeping the pad block firmly attached to the fingertip.

The structures of the mechanical links for each finger are the same except for the thumb. Due to the unusual geometry of the thumb joint and large workspace, the three-linkage design is not possible to comfortably and repeatedly secure an exoskeleton mechanism to the proximal link. Thus, one more link was added to the thumb base to decouple several off-axis rotations as shown in Fig. 1 (denoted by "Link 0").

Through study of anthropomorphic data and optimization analysis [44], we selected optimum linkage lengths for each link of the glove mechanism. Because a single actuator drives the three links, this property not only makes the glove simpler and lighter, but it also allows the finger mechanism to be self-adapting to different finger sizes. The kinematic analysis of the glove mechanism detail can be found in Appendix.

B. Electrical Design

The block diagram of the electrical system design for this device is shown in Fig. 3. The system is composed of a host unit and a portable haptic glove. The host unit is made up of a wireless RF transmitter (XBee, which is compact in size and easy to use. Its 1 mW transmission power at 2.4GHz provides 30 m working range indoors) and a PC which collects, records and displays the joint angles and force measurements, while simultaneously sending the control data back to the glove system. The haptic system includes a glove skeleton and an electrical control interface.

The focus of the electronics is on the development of a circuit interface board (Fig. 4) in a compact size, which incorporates 21-channel A/D converter (15 for finger joint sensors and

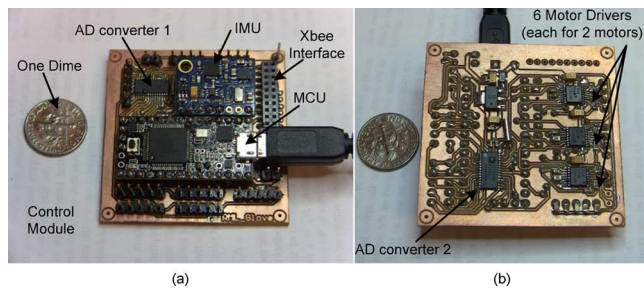


Fig. 4. Custom PCB design, (a) top view, (b) bottom view.

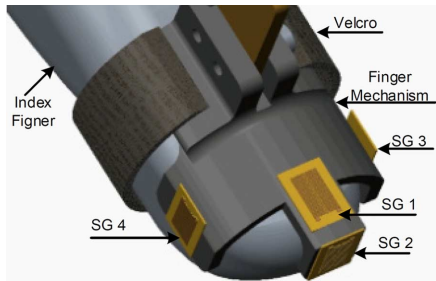


Fig. 5. Location of strain gauge sensors at the fingertip mechanism.

6 for motor current measurement), 5 differential input channels, 1 dual/differential 16-to-1 channel multiplexer, 6 dc motor drivers, a wireless module and a microcontroller.

To reduce the complexity of the mechanical and electrical construction between the fingers and maximize the finger workspace, two customized PCBs with mounted three angular position encoders (Hall element sensor EM-3242) are used as the two links of the finger mechanism (Link1 and Link3, as shown Fig. 1). The three angular encoders (two on Link 1 and one on Link 3) provide accurate joint angle measurements for calculating each finger's configuration and position. After calibration, the joint rotation resolution of the Hall-effect rotation sensor was experimentally determined to be 0.37° . The joint angle error was less than 0.8% of the total range of motion (120°) and the error was well below the Just Noticeable Difference (JND) of proximately 2.5° for the PIP and MCP joints [45]. Thus, no extra angular encoder sensors are needed to be attached to the joint. These encoders are soldered directly onto the PCB board, which is used as both a mechanical link and a carrier of electrical components and signals. This dual function makes the glove mechanism lighter without sacrificing strength. Strain Gauge sensors were used to measure contact forces, which are mounted on the fingertip pad, as shown in Fig. 5. The fingertip mechanism was designed to be slightly smaller than medium sized fingers and it can be easily bent to adapt to different finger sizes. Strain was measured along the longitudinal and the transverse axes using pseudo-differential input channel of a sensor interface (Analog Devices, Inc., AD7708). Motor current is also measured through a shunt circuit on the custom PCB. Thus, both joint angle and torque/force measurements are collected for feedback control and for data analysis.

The control module is a MK20DX128 microcontroller (32 bit ARM Cortex-M4 by Freescale) used to manage the sensor

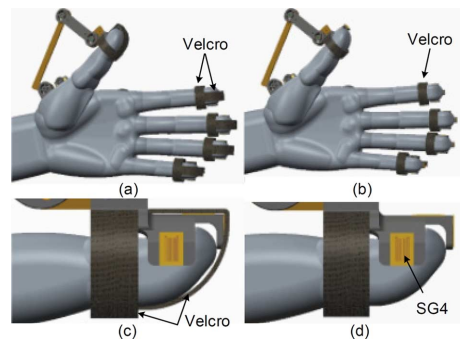


Fig. 6. Two modes of measuring force: (a) and (c) Haptic mode—measuring the force between the glove and fingers; (b) and (d) Record mode—measuring the force between the fingers and the object.

measurement, which performs several functions: reading and conditioning the sensor data, controlling the force magnitude applied at the user's fingertips through controlling the motor rotation, and communicating with the host unit. In this case, the microcontroller speed is set to 96 MHz. Additionally, software running on the control module conditions the rotation and force signals with low pass filters with a cutoff frequency of 10 Hz, converts them into human joint angles and calibrates forces in less than 1 ms and transmits the data through a wireless module with an update rate of 100 Hz.

The battery used was the Powerizer LI-9V400 (9 V, 400 mAh, dimensions $48 \times 26 \times 16$ mm, with 20 g of weight), which can last as long as 70 min under continuous operation (average power consumption of the whole system is about 300 mA). Communication between the haptic glove and host computer is accomplished through wireless RF modules. The wireless transmission speed is 115 200 bits/s. The transmitted data from the haptic glove contains finger joint angles and measured fingertip contact forces. The data that the haptic glove receives includes motor speed and forces to be applied to the operator's finger. The adoption of the RF module and the compact mechanical and electrical design made the glove wireless, portable and self-contained.

C. Measuring Force

It has been known that during grasping, the main contact forces between the fingers and the objects are normal to the fingertip surface [46], [47]. Some applications, such as VR, teleoperation grasping and rehabilitation engineering, consider forces in this direction the most useful. Thus the fingertip force sensors mainly sense the actual force applied by the fingertip in this direction. The locations of touch sensors at the fingertip mechanism are shown in Fig. 5. Four Strain Gauge (SG) sensors are used to constitute a force-sensing platform to measure the fingertip force in two different modes: Haptic Mode and Record Mode.

Fig. 6 shows the differences between the two modes, with or without the Velcro attached to the fingertip. It is easy and quick to switch between the two modes, since only a piece of Velcro needs to be removed or attached.

In the Haptic Mode, only SG1 is used to measure the force between the fingertip and the haptic glove. As shown in Fig. 6(c),

when the hand bends, the Velcro pulls SG1. When the hand extends, the fingertip pushes the mechanism, thus SG1 bends in the opposite direction. The contact force, between the finger and the mechanism, is then acquired. These force signals are fed back to the microcontroller which controls the actuator to make appropriate adjustments, such that the desired force profile is perceived by the user. In Haptic Mode, 5 SG1 sensors on five fingers were directly connected to the five pseudo-differential input channels.

In the Record Mode, the SAFE Glove is adapted to a demonstration device to record the measurement of finger and thumb joint angles, and finger pressures associated with common movements of hand functions including grip and release patterns. Similar to [30], SG 2, SG3 and SG4 are used to measure the force between the fingertip and the object in Record Mode. The contact force was obtained by averaging all the three force values. 15 strain gauge sensors (SG2, SG3 and SG4 on each finger) were connected to a dual /differential 16-to-1 channel multiplexer, which was connected to the pseudo-differential input channel. When the contact force increases, the fingertip pad deforms more and the force sensors can pick up this change through the bending of the glove mechanism. Without the Velcro on the fingertip, nothing inhibits the tactile sensation since the pad of the fingertip is exposed to allow the user to feel the texture of different objects directly. As discussed in the first section, it is better to allow the finger direct contact with the object. Evaluation results of those two modes are shown in Section IV.

III. WORKSPACE ANALYSIS OF HAND AND GLOVE

A. Human Factor

The human hand is one of the main organs for us to interact with the environment. Each hand contains approximately 29 bones and 34 muscles to move all the fingers [1]. Such high degrees of freedom and massive neural connections provide an enormous flexibility to perform all kinds of finger movements, such as touch, press, grasp, squeeze, throw, etc. On the other hand, the complex mechanical property makes modeling the hand kinematics and hand motion a challenging problem for researchers [49]. The precise teleoperation, VR and rehabilitation tasks of haptic gloves require an accurate hand model (i.e., finger length and joints location) in order to achieve an accurate control and reduce the motion sensing errors.

The interactions between the kinematics of the hand and the size of the glove have a great effect on hand gesture and grip force. Haptic gloves need to be designed for both convenient and safe use. The glove workspace should ideally cover the entire hand workspace. The detailed kinematic analysis can be found in [41].

B. Hand Workspace Analysis

One major challenge in artificially generating haptic sensations is that haptic gloves should allow the user to make desired motions without restricting the operator's motion, thus requiring back-drivability and sufficient degrees of freedom of motion. The anthropometric data of the average length for each finger phalangeal segments are listed in Table I based on [50]–[53].

TABLE I
PHALANX LENGTH OF EACH FINGER (MM)

Finger	Proximal Phalanx	Middle Phalanx (Metacarpal for Thumb)	Distal Phalanx
Index	48.3	28.2	19.1
Middle	52.4	33.5	21.3
Ring	48.1	32.5	21.1
Little	40.2	23.0	18.3
Thumb	38.6	49.4	31.1

TABLE II
FINGER JOINT MOTION RANGES

Finger	Angular Motion Range (Degree)
MCP FE	[-90, 30]
MCP AA	[-20, 20]
PIP FE	[-100, 0]
DIP FE	[-70, 5]
Thumb CMC FE	[-100, 10]
Thumb CMC AA	[-100, 0]
Thumb MCP FE	[-90, 10]
Thumb IP FE	[-90, 20]

This data and information are used as design parameters of the haptic glove. The data is also used to calculate the workspaces of each finger.

Regarding the motion ranges of each finger joint, the authors did not find similar detailed anthropometric data available in the medical literature, but only some limited studies were published [54]–[56]. In order to make the glove design adaptable to larger populations, the union of all of the above collection sets was combined to calculate the workspace of each finger. The combined motion ranges are shown in Table II.

MATLAB Robotics Toolbox [57] was used to model both the human hand and the haptic glove. Each finger was created as serial kinematically-rigid robots, using the standard Denavit-Hartenberg (DH) notation. Based on this toolbox, when the joint angles vary through their known ranges, point clouds are generated inside the workspace. Alpha-shape method [58] was adopted to calculate the workspace volume based on those points cloud. Based on the finger length and joint ranges of motion defined in Tables I and II, the 3D workspace for all the fingers can be obtained, as shown in Fig. 7. As the figure illustrates, the thumb workspace intersects with all the other fingers workspaces, implying that the workspace analysis should be correct.

C. Workspace Analysis of SAFE Glove

Since most of the human hand activity depends on the movements of the thumb and the index finger, the workspace of these two fingers for both the glove and the hand is analyzed in this subsection. According to the four-linkage mechanism model [41], and the optimized link lengths and joint motion ranges as depicted in [42] [link length = [73.88; 47.23; 19.1] (mm), $\alpha_1 = [-80, 60]$, $\alpha_2 = [-130, -50]$, $\alpha_3 = [-80, 60]$ (degree)], the 3D workspace for the index finger can be obtained, as shown in Fig. 8 (human finger workspace is also included for comparison). Similarly, the thumb mechanism and the thumb finger

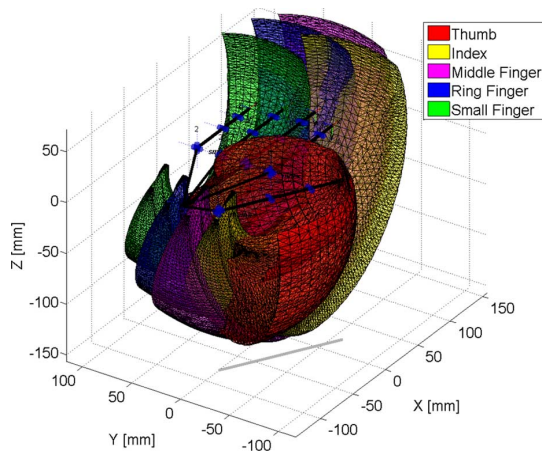
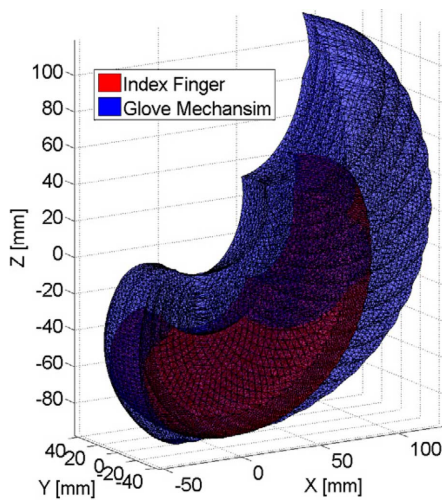
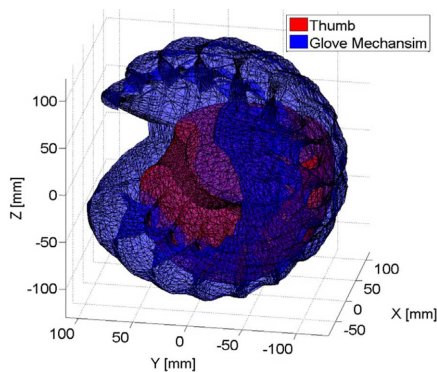


Fig. 7. Workspace of all five fingers.

Fig. 8. Workspace of the index finger (finger workspace: $3.58 \times 10^5 \text{ mm}^3$, Glove workspace: $7.71 \times 10^5 \text{ mm}^3$).Fig. 9. Workspace of the thumb. (Thumb workspace: $1.12 \times 10^6 \text{ mm}^3$, Glove thumb mechanism: $3.44 \times 10^6 \text{ mm}^3$).

workspace are shown in Fig. 9. As Figs. 8 and 9 illustrate, the finger workspace is a subset of the mechanism's workspace for both index and thumb fingers, ensuring the glove allows unimpeded finger motion. This means that the new mechanism design should ideally cover this entire workspace. Similar results are seen for the workspaces of the other fingers and mechanisms.

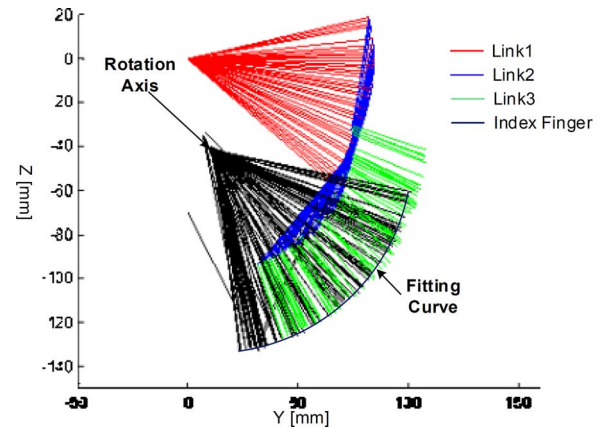


Fig. 10. Finger length measurement.

IV. EXPERIMENTAL RESULTS

A. Finger Length Measurement

It is fundamental to measure the finger position and orientation quantitatively for hand motion analysis. While assessing the hand function, besides the finger joints, the finger length information is also required. During the measurement stage, finger length and joint angles are the most essential factors. However, most of the previously mentioned research is mainly focused on measuring the finger joint angles during a specific movement. There is still lack of studies aimed at analyzing finger length, which highly affects the fingertip position. Since finger rotation axes are difficult to locate, the length of the finger is prone to artifacts. Thus, improving finger length measurement accuracy is required. The authors then propose a novel measurement method which uses haptic-glove on an articulated hand model to determine finger lengths from multiple movements [60].

The glove design allows an individual to place the glove on their hand and get actual finger angles regardless of the hand size. Thus, the key elements of modeling the hand are: 1) to measure the length of the user's fingers, which directly takes input from the individual user, 2) to map the mechanism joint positions directly into human finger angles through forward and inverse kinematics based on the finger length and fixed glove mechanism geometries.

The proposed solution determines the finger length parameters using a circle fitting procedure from a collection of points with the five-fingered glove mechanism. In this experiment, only planar movements are considered and the axis of rotation is supposed to be perpendicular to the plane of motion. After wearing the glove, the user is asked to rotate the MCP joint of the finger in flexion/extension direction while keeping the PIP and DIP joints at zero degrees as much as possible. Concurrently, the glove records the fingertip curve-like trajectory. The method of least squares fitting of circles is used to analyze the kinematic model. The experimental result is shown in Fig. 10.

According to [59], lengths of three phalangeal segments of each finger are approximated by a "Fibonacci" sequence (i.e., 2, 3, 5, 8) from distal to proximal. Thus, the length of each phalanx is the sum of lengths of the other two distal segments. Following this relationship, the length of each phalangeal segment can be

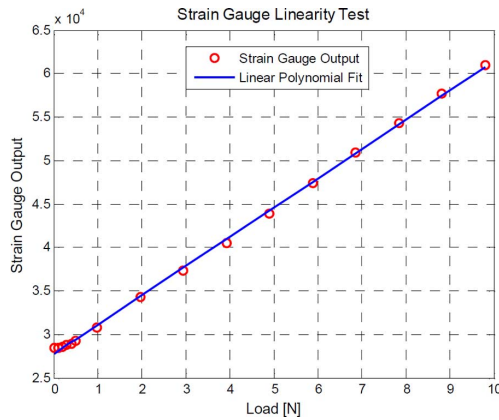


Fig. 11. Strain gauge # 1 linearity test.

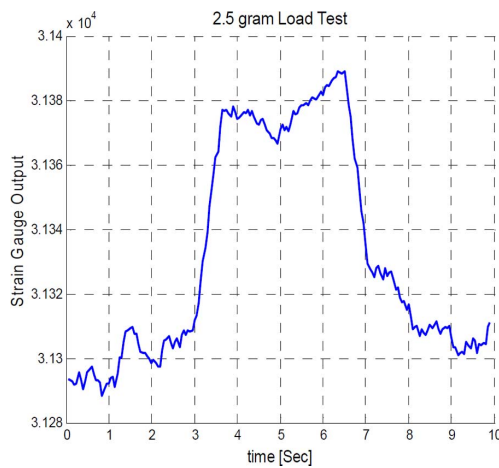


Fig. 12. Minimum load test.

calculated. The finger length results may be stored to allow the same user to use the device again without recalibration.

According to [59], lengths of three phalangeal segments of each finger are approximated by a “Fibonacci” sequence (i.e., 2, 3, 5, 8) from distal to proximal. Thus, the length of each phalanx is the sum of lengths of the other two distal segments. Following this relationship, the length of each phalangeal segment can be calculated. The finger length results may be stored to allow the same user to use the device again without recalibration.

B. Strain Gauge #1 Calibration

In the Haptic Mode, to experimentally simulate the normal force applied to the fingertip mechanism, different weights were suspended from the Velcro. Fig. 11 shows the calibration result for SG1 output over a range of 0–1000 g weight.

The force measurement linearity was less than 2.17% of the total range (0–10N). Due to the inflexibility of the Velcro, the maximum error occurs when the load gets close to zero. If the first two points (Load = 0 and 0.1N) were removed, the linearity becomes 0.73%.

In the Haptic Mode, the output resolution of the SG1 sensor was experimentally determined to be 2.5 g, as shown in Fig. 12. For the Haptic Mode, no calibration process is required for different users when the SAFE Glove was calibrated.

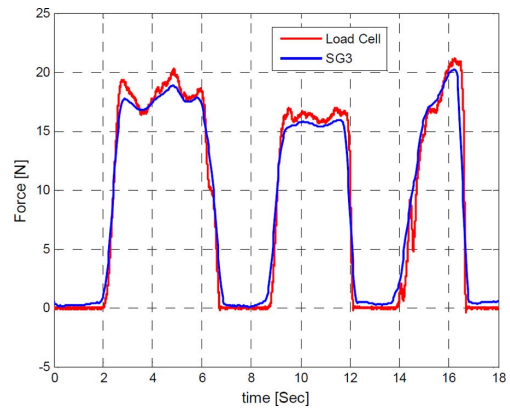


Fig. 13. Contact force measurement experiment.

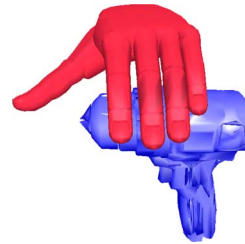


Fig. 14. 3D GUI of hand kinematics.

C. Contact Force Measurement Experiment

A Load Cell (MLP-10, Transducer Techniques, Inc.) was used to perform a comparative experiment with the force readings from the glove. The Load Cell was amplified and conditioned by the signal conditioner (TM0–2, Transducer Techniques, Inc). Consequently, the Load Cell measurements are used as reference for comparison. The SG sensors on the fingertip were sampled by the 16-bit fully differential input channels at 100 Hz on the customized PCB. A low-pass filter was implanted in the software to condition the SG output. The measured force and SG data of the finger pad were simultaneously collected and recorded on a desktop computer.

In the contact force measurement experiment, after wearing the SAFE Glove, the participant was asked to place the index finger pad on top of the Load Cell and applied force three times in about 20 s. As shown in Fig. 13, a typical experimental result shows that the load cell output curve is analogous to the normalized contact force measured by SG3 (SG2 and SG4 have similar results to SG3, thus they are not shown). The method of least squares was used to normalize the sensor output. Fig. 13 shows that it is feasible to measure the net contact force applied to the fingertip through the SAFE Glove.

D. Assisting Hand Motion Experiments

On the host unit, a 3D GUI was programmed based on an open-source framework for haptics and dynamics simulations (CHAI 3D [61]) with C++ to show the hand kinematics in real time. The GUI can display the posture of fingers and record the positions of the fingertip with three DOF (MCP, PIP, and DIP joints) for each finger as shown in Fig. 14. Experiments to assist hand motions were performed to evaluate the effectiveness of the proposed glove.

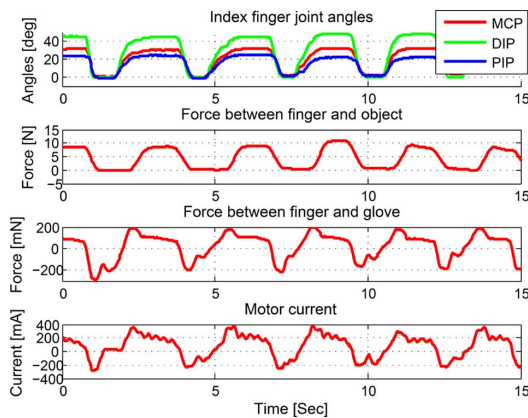


Fig. 15. Index finger motion during grasping a bottle of water.

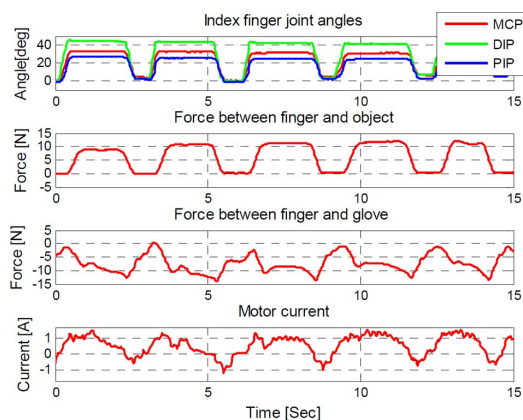


Fig. 16. Index finger motion during assisting grasping of a bottle.

The first step of this experiment is to record joint motions and finger pressures in the pick-and-place task. The task includes the procedure of gripping, lifting, placing and releasing. Two objects, a 500 g bottle of water and a 200 g apple, were tested in this experiment. In this step, the glove was controlled to follow the fingers movement by minimizing the force between the finger and the glove throughout the motion. After getting used to wearing the SAFE Glove, the participant was asked to repeat the pick-and-place tasks five times in about 15 s. As a representative example of the test results, the index finger motion result in grasping a bottle of water test is shown in Fig. 15.

The second step is to generate these movement patterns in playback fashion to assist a “weakened” hand to accomplish these movements. Since the user has a pair of healthy hands, he was asked to passively follow the glove movement without applying any active force. The glove was programmed to actively drive the user’s fingers to follow the position and force trajectory from the recorded data. Similarly, the index finger motion result is shown in Fig. 16. The other fingers motions have similar results and the apple grasping experiment is similar to the bottle grasping test. Both Figs. 15 and 16 display similar joint angle trajectories and contact force between the finger and object, which demonstrate that the glove was controlled smoothly and effectively. Regarding the force between the finger and the glove shown in the third row, Fig. 16 differs

from Fig. 15 in terms of both direction and amplitude. Apparently, in the recording step (Fig. 15), the direction of this force is always opposite to the direction of the finger movement due to the inertial and friction effects of the mechanism. Our control algorithm minimizes this force to less than 200 mN [41]. In the assistance step experiment, this force is used to drive the hand motion, thus the force direction is always the same as the direction of the finger movement and the amplitude is as high as 10 N. The similar relations can also be found in the motor current signal shown in the fourth row of Fig. 16. The experimental results validate that the newly designed five-fingered glove is capable of reliably recording and assisting the hand function in daily grasping movements.

V. CONCLUSION AND FUTURE WORK

This paper proposed a new haptic device that is designed to gather kinematic and force information of the user’s hand and to play back the motion to assist the user in common hand grasping movements, such as grasping a bottle of water or an apple.

Moreover, the glove system architecture was also presented. The lightweight self-contained glove is adaptable to a wide variety of finger sizes without constraining the range of the fingers’ motion. With this glove system, the finger length information can be acquired easily and intuitively so that the joint angle for different subjects can be calculated through forward and inverse kinematics.

The primary advantages of the SAFE Glove are as follows. First, it is light-weight which reduces user fatigue and the wireless communication capability with a PC or a mobile robot [62]–[64] greatly increases its portability. Second, the mechanical design is compact without limiting the natural ranges of motion of human fingers. Third, it can accurately measure the hand kinematics and provide force feedback information. Fourth, the SAFE Glove is inexpensive. Furthermore, the system is safe to the user and it can last over one hour of continuous operation before the need to recharge.

Future work includes adding an Inertial Measurement Unit that is composed of accelerometers, gyroscopes and magnetometers to the glove system to facilitate the measurement of the whole hand position and orientation, such that the system can be used for rehabilitation applications or be integrated with virtual reality environments.

Ongoing mechanical refinement of this device is being directed towards the use of smaller and stronger components to reduce bulkiness and improve comfort for the wearer. Later generation designs will consist of gloves pulled directly over the hand with all operational components closely fitted to the dorsum. Concurrently, refinement of our computer database will be directed to more elegant organization of the higher order movement variables, allowing faster feed-back to the system motors and also for greater ease of use with future experiments.

On a larger scale the techniques developed in this research project will mimic the brain-muscle interface of human movement patterns enabling the cataloging of normal hand function (movement), thereby creating a data base which will be useful for many future studies of functional hand movement.

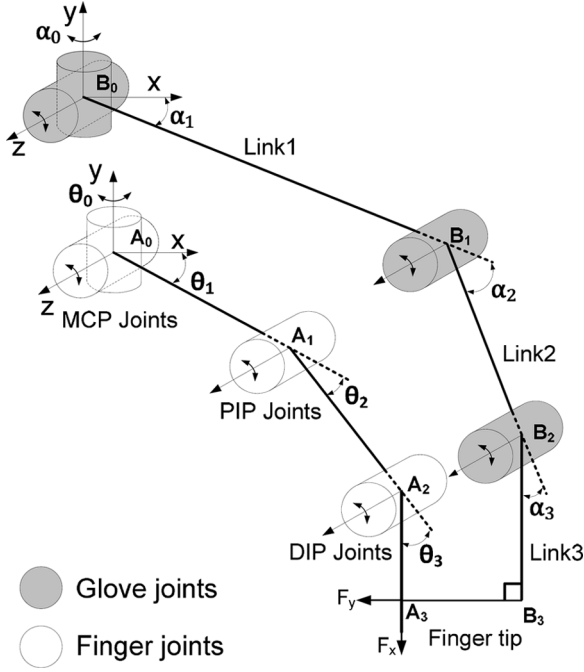


Fig. 17. Kinematic diagram of the finger/glove system.

APPENDIX KINEMATIC ANALYSIS

For each finger, the haptic mechanism and the finger itself can be modeled as a single six-bar mechanism, as shown in Fig. 17, where the hand/support pad represents the ground. Each finger has three links, and the haptic mechanism has three links, too. However, the terminal link of each finger is rigidly connected to the terminal link of the haptic mechanism through the Velcro strap discussed in Section II. Therefore, there are six links in total (one ground, three finger links, two haptic mechanism links) and six revolute pin connections (ignoring the adduction/abduction due to its relative small range). According to Grubler's formula, the mobility of the system can be calculated using (1), where DF is the system's degrees of freedom (DOF), n is the number of links, f_1 is the number of lower-pair (1 DOF) joints, and f_2 is the number of higher-pair (2 DOF) joints

$$DF = 3(n - 1) - 2f_1 - f_2 = 3. \quad (1)$$

Based on Fig. 17, equations for the fingertip position (x_{A3}, y_{A3}) and angle ϕ are derived in (2)–(4) in terms of the finger joint angles $(\theta_1, \theta_2, \theta_3)$ and the mechanism joint angles $(\alpha_1, \alpha_2, \alpha_3)$, where l_i is the length of the i^{th} mechanism link $\overline{B_{i-1}B_i}$, p_i is the length of the i^{th} finger link $\overline{A_{i-1}A_i}$, l_p is the length of $\overline{B_3A_3}$. In addition, s and c represent sine and cosine, such that $C_{\alpha,12}$ is $\cos(\alpha_1 + \alpha_2)$

$$\begin{aligned} x_{A3} &= x_{B0} + l_1 c_{\alpha,1} + l_2 c_{\alpha,12} + l_3 c_{\alpha,123} + l_p c_{(90+\alpha,123)} \\ &= p_1 c_{\theta,1} + p_2 c_{\theta,12} + p_3 c_{\theta,123} \end{aligned} \quad (2)$$

$$\begin{aligned} y_{A3} &= y_{B0} + l_1 s_{\alpha,1} + l_2 s_{\alpha,12} + l_3 s_{\alpha,123} + l_p s_{(90+\alpha,123)} \\ &= p_1 s_{\theta,1} + p_2 s_{\theta,12} + p_3 s_{\theta,123} \end{aligned} \quad (3)$$

$$\phi = \alpha_1 + \alpha_2 + \alpha_3 = \theta_1 + \theta_2 + \theta_3. \quad (4)$$

After solving (2)–(4), the mechanism joint angles α_1, α_2 and α_3 may be calculated using (5)–(7). The finger angles θ_1, θ_2 and θ_3 are prescribed by the user

$$\alpha_1 = \arctan\left(\frac{N}{M}\right) + \arccos\left(\frac{p_1^2 + p_2^2 + N^2 - M^2}{2p_1\sqrt{M^2 + N^2}}\right) \quad (5)$$

$$\alpha_2 = \arccos\left(\frac{M^2 + N^2 - p_1^2 - p_2^2}{2p_1 p_2}\right) \quad (6)$$

$$\alpha_3 = \theta_1 + \theta_2 + \theta_3 - \alpha_1 - \alpha_2 \quad (7)$$

where:

$$M = -x_{B0} + l_1 c_{\theta,1} + l_2 c_{\theta,12} + (l_3 - p_3) c_{\theta,123} + l_p s_{\theta,123}$$

$$N = -y_{B0} + l_1 s_{\theta,1} + l_2 s_{\theta,12} + (l_3 - p_3) s_{\theta,123} + l_p c_{\theta,123}.$$

Conversely, if the mechanism joint angles are known, by a similar analysis, the exact finger position can be calculated, which can then be used in applications such as medical training, tele-operation, etc.

REFERENCES

- [1] R. Tubiana, J. Thomine, and E. Mackin, *Examination of the Hand & Upper Limb*. Philadelphia, PA: WB Saunders, 1984, p. 79.
- [2] L. A. Jones and S. J. Lederman, *Human Hand Function*. Oxford, U.K.: Oxford Univ. Press, 2006, p. 7.
- [3] J. Blake and H. B. Gurocak, "Haptic glove with MR brakes for virtual reality," *IEEE/ASME Trans. Mechatron.*, vol. 14, no. 5, pp. 606–615, Oct. 2009.
- [4] V. Popescu, G. Burdea, and M. Bouzit, "Virtual reality simulation modeling for a haptic glove," in *Proc. IEEE Comput. Animat.*, 1999, pp. 195–200.
- [5] M. Bouzit, G. Burdea, G. Popescu, and R. Boian, "The Rutgers master II- new design force-feedback glove," *IEEE/ASME Trans. Mechatron.*, vol. 7, no. 2, pp. 256–263, Jun. 2002.
- [6] S. Lichiardopol, A survey on teleoperation Dept. Mech. Eng., Dynamics Control Group, Tech. Univ. Eindhoven, Eindhoven, The Netherlands, Tech. Rep. DCT2007.155, 2007.
- [7] J. Park and O. Khatib, "A haptic teleoperation approach based on contact force control," *J. Robot. Res.*, vol. 25, pp. 575–591, 2006.
- [8] F. Kobayashi, G. Ikai, W. Fukui, and F. Kojima, "Two-fingered haptic device for robot hand teleoperation," *J. Robot.*, 2011.
- [9] A. V. Chiri *et al.*, "Mechatronic design and characterization of the index finger module of a hand exoskeleton for post-stroke rehabilitation," *IEEE/ASME Trans. Mechatron.*, vol. 17, no. 5, pp. 884–894, Oct. 2012.
- [10] S. Ueki *et al.*, "Development of a hand-assist robot with multi-degrees-of-freedom for rehabilitation therapy," *IEEE/ASME Trans. Mechatron.*, vol. 17, no. 1, pp. 136–146, Feb. 2010.
- [11] L. Connelly *et al.*, "A pneumatic glove and immersive virtual reality environment for hand rehabilitative training after stroke," *IEEE Trans. Neural Syst. Rehabil. Eng.*, vol. 18, no. 5, pp. 551–559, Oct. 2010.
- [12] L. Dipietro, A. Sabatini, and P. Dario, "A survey of glove-based systems and their applications," *IEEE Trans. Syst., Man, Cybern., C*, vol. 38, no. 4, pp. 461–482, Jul. 2008.
- [13] M. Bianchi, P. Salaris, A. Turco, N. Carbonaro, and A. Bicchi, "On the use of postural synergies to improve human hand pose reconstruction," in *IEEE Haptics Symp.*, 2012, pp. 91–98.
- [14] M. Borghetti, E. Sardini, and M. Serpelloni, "Sensorized glove for measuring hand finger flexion for rehabilitation purposes," *IEEE Trans. Instrum. Meas.*, vol. 62, no. 12, pp. 3308–3314, Dec. 2013.
- [15] H. Liu, "Exploring human hand capabilities into embedded multifingered object manipulation," *IEEE Trans. Ind. Informat.*, vol. 7, no. 3, pp. 389–398, Aug. 2011.
- [16] C. Metcalf, S. Notley, P. Chappell, J. Burrige, and V. Yule, "Validation and application of a computational model for wrist movements using surface markers," *IEEE Trans. Biomed. Eng.*, vol. 55, no. 3, pp. 1199–1210, Mar. 2008.
- [17] I. Carpinella, J. Jonsdottir, and M. Ferrarin, "Multi-finger coordination in healthy subjects and stroke patients: A mathematical modelling approach," *J. Neuroeng. Rehabil.*, vol. 8, no. 19, 2011.

- [18] A. Erol, G. Bebis, M. Nicolescu, R. Boyle, and X. Twombly, "Vision-based hand pose estimation: A review," *Comput. Vis. Image Understand.*, vol. 108, no. 1–2, pp. 52–73, 2007.
- [19] M. Gorce, D. Fleet, and N. Paragios, "Model-based 3D hand pose estimation from monocular video," *IEEE Trans. Pattern Anal. Mach. Intell.*, vol. 33, no. 9, pp. 1793–1805, Sep. 2011.
- [20] A. Erol, G. Bebis, M. Nicolescu, R. D. Boyle, and X. Twombly, "A review on vision-based full DoF hand motion estimation," in *Proc. Workshop Vis. Human-Comput. Interact.*, Jun. 2005.
- [21] V. F. Pamplona, L. A. Fernandes, J. L. Prauchner, L. P. Nedel, and M. Oliveira, "The image-based data glove," in *Proc. 10th Symp. Virt. Augment. Reality*, 2008.
- [22] A. Agur and M. Lee, *Grant's Atlas of Anatomy*, 10th ed. Philadelphia, PA: Lippincott Williams Wilkins, 1999.
- [23] E. Komi, J. Roberts, and S. Rothberg, "Evaluation of thin, flexible sensors for time-resolved grip force measurement," *IMECH Part C: J. Mech. Eng. Sci.*, vol. 221, pp. 1687–1699, 2007.
- [24] L. Paredes-Madrid and P. G. d. Santos, "Dataglove-based interface for impedance control of manipulators in cooperative human-robot environments," *Meas. Sci. Technol.*, vol. 2, 2013.
- [25] W. Walsh *et al.*, "Proprioceptive signals contribute to the sense of body ownership," *J. Physiol.*, pp. 3009–3021, 2011.
- [26] J. Li, M. R. Cutkosky, J. Ruutiainen, and R. Raisamo, "Using haptic feedback to improve grasp force control in multiple sclerosis patients," *IEEE Trans. Robot.*, vol. 25, no. 3, pp. 593–601, Jun. 2009.
- [27] A. Mascaro and H. Asada, "Photoplethysmograph fingernail sensors for measuring finger forces without haptic obstruction," *IEEE Trans. Robot. Automat.*, vol. 17, no. 5, pp. 698–708, Oct. 2001.
- [28] Y. Sun, J. Hollerbach, and S. Mascaro, "Estimation of finger force direction with computer vision," *IEEE Trans. Robot.*, vol. 25, no. 6, pp. 1356–1369, 2009.
- [29] Y. Watanabe, Y. Makino, K. Sato, and T. Maeno, "Contact force and finger angles estimation for touch panel by detecting transmitted light on fingernail," in *Haptics: Perception, Devices, Mobility, and Communication*. Berlin, Germany: Springer, 2012, pp. 601–612.
- [30] M. Nakatani, K. Shiojima, and S. Kinoshita, "Wearable contact force sensor system based on finger pad deformation," in *4th Joint EuroHaptics Conf. IEEE Haptics*, Istanbul, Turkey, Jun. 2011, pp. 323–328.
- [31] T. Endo, M. Kobayashi, and H. Kawasaki, "A finger skill transfer system using a multi-fingered haptic interface robot and a hand motion image," *Robotica*, vol. 31, no. 8, pp. 1–11, 2013.
- [32] L. Dovat *et al.*, "Handcare: A cable-actuated rehabilitation system to train hand function after stroke," *IEEE Trans. Neural Syst. Rehabil. Eng.*, vol. 16, no. 6, pp. 582–591, Dec. 2008.
- [33] H. Fang, Z. Xie, and H. Liu, "An exoskeleton master hand for controlling DLR/HIT hand," in *IEEE/RSJ, Conf. Intell. Robots Syst.*, Oct. 2009, pp. 3703–3708.
- [34] S. H. Winter and M. Bouzit, "Use of magnetorheological fluid in a force feedback glove," *IEEE Trans. Neural Syst. Rehabil. Eng.*, vol. 15, no. 1, pp. 2–8, Mar. 2007.
- [35] K. Tong *et al.*, "An intention driven hand functions task training robotic system," in *Proc. Annu. Int. Conf. IEEE Eng. Med. Biol. Soc.*, Sep. 2010, pp. 3406–3409.
- [36] J. Arata *et al.*, "A new hand exoskeleton device for rehabilitation using a three-layered sliding spring mechanism," in *Proc. IEEE Int. Conf. Robot. Automat.*, Karlsruhe, Germany, May 6–10, 2013, pp. 3887–3892.
- [37] T. Koyama, K. Takemura, and T. Maeno, "Development of an ultrasonic clutch, ultrasonics," in *IEEE Symp.*, 2003, vol. 1, pp. 597–600.
- [38] A. Heuser *et al.*, "Telerehabilitation using the Rutgers master II glove following carpal tunnel release surgery: Proof-of-concept," *IEEE Trans. Neural Syst. Rehabil. Eng.*, vol. 15, no. 1, pp. 43–49, Mar. 2007.
- [39] *CyberGrasp Manual, V2.0*. San Jose, CA: Immersion, 2007.
- [40] Anderson and J. Robert, Advanced dexterous manipulation for IED defeat: Report on the feasibility of using the shadowhand for remote operations Sandia Nat. Lab., Rep. SAND2011–0438., 2011.
- [41] Z. Ma and P. Ben-Tzvi, "RML glove—An exoskeleton glove mechanism with haptics feedback," *IEEE/ASME Trans. Mechatron.*, 20, no. 2, pp. 641–652, Apr. 2015.
- [42] I. Kapandji, *The Physiology of the Joints*. London, U.K.: Churchill Livingstone, 2007, vol. 1.
- [43] A. H. A. Stienen, E. E. G. Hekman, F. C. T. V. D. Helm, and H. V. D. Kooij, "Self-aligning exoskeleton axes through decoupling of joint rotations and translations," *IEEE Trans. Robot.*, vol. 25, no. 3, pp. 628–633, Jun. 2009.
- [44] Z. Ma and P. Ben-Tzvi, "Design and optimization of a five-finger haptic glove mechanism," *J. Mechan. Robot.*
- [45] RLE Progress Rep. Massachusetts Inst. Technol., 135, 1992, p. 305 [Online]. Available: <http://www.dtic.mil/dtic/tr/fulltext/u2/a266730.pdf>
- [46] S. Springer and R. Gadh, "Haptic feedback for virtual reality computer aided design," *ASME Int. Mech. Eng. Congr. Expo.*, Nov. 1997.
- [47] S. L. Springer and N. J. Ferrier, "Design and control of a force-reflecting haptic interface for teleoperational grasping," *Trans. ASME J. Mech. Design*, vol. 124, no. 2, pp. 277–283, Jun. 2002.
- [48] Z.-H. Mao, H.-N. Lee, R. J. Sclabassi, and M. Sun, "Information capacity of the thumb and the index finger in communication," *IEEE Trans. Biomed. Eng.*, vol. 56, no. 5, pp. 1535–1545, May 2009.
- [49] A. Murgia, "A gait analysis approach to the study of upper limb kinematics using activities of daily living," Ph.D. dissertation, Univ. Reading, Reading, U.K., 2005.
- [50] A. Freivalds, *Biomechanics of the Upper Limbs: Mechanics, Modeling, and Musculoskeletal Injuries*. Boca Raton, FL: CRC Press, 2004.
- [51] E. M. Churchill and T. John, "Sampling and data gathering strategies for future USAF anthropometry," *A/F Aerospace Med. Res.* 2–76, pp. 121–128, 1976.
- [52] NASA: Space flight human system standard volume 2: Human factors, habitability, and environmental health, NASA-STD-3001 2010 [Online]. Available: URL:<http://msis.jsc.nasa.gov/>
- [53] B. Buchholz, T. J. Armstrong, and S. A. Goldstein, "Anthropometric data for describing the kinematics of the human hand," *Ergonomics*, vol. 35, no. 3, pp. 261–273, 1992.
- [54] J. A. Buckwalter, T. A. Einhorn, and S. R. Simon, *Orthopaedic Basic Science: Biology and Biomechanics of the Musculoskeletal System*. Rosemont, IL: Am. Acad. Orthopaedic, 2000, vol. 1.
- [55] J. E. Muscolino, *Kinesiology: The Skeletal System and Muscle Function*. St. Louis, MO: Mosby Elsevier, 2006.
- [56] H. L. Yu, R. A. Chase, and B. Strauch, *Atlas of Hand Anatomy and Clinical Implications*. St. Louis, MO: Mosby, 2004.
- [57] P. I. Corke, *Robotics, Vision & Control: Fundamental Algorithms in MATLAB*. New York: Springer, 2011.
- [58] H. Edelsbrunner, D. G. Kirkpatrick, and R. Seidel, "On the shape of a set of points in the plane," *IEEE Trans. Inform. Theory*, vol. 29, no. 4, pp. 551–559, Jul. 1983.
- [59] A. Buryanov and V. Kotiuk, "Proportions of hand segments," *Int. J. Morphol.*, vol. 28, no. 3, pp. 755–758, 2010.
- [60] Z. Ma and P. Ben-Tzvi, "Modeling human hand and sensing hand motions with the five-fingered haptic glove mechanism," in *Proc. ASME IDETC/CIE, Conf. Mech. Robot.*, Aug. 2014.
- [61] F. Conti, F. Morris, D. Barbagli, and F. Sewell, C.: Chai 3D 2006 [Online]. Available: <http://www.chai3d.org>
- [62] P. Ben-Tzvi, A. A. Goldenberg, and J. W. Zu, "Design and analysis of a hybrid mobile robot mechanism with compounded locomotion and manipulation capability," *Trans. ASME, J. Mech. Design*, vol. 130, no. 7, pp. 1–13, Jul. 2008.
- [63] P. Ben-Tzvi, "Experimental validation and field performance metrics of a hybrid mobile robot mechanism," *J. Field Robot.*, vol. 27, no. 3, pp. 250–267, May 2010.
- [64] P. Ben-Tzvi, A. A. Goldenberg, and J. W. Zu, "Articulated hybrid mobile robot mechanism with compounded mobility and manipulation and on-board wireless sensor/actuator control interfaces," *Mechatron. J.*, vol. 20, no. 6, pp. 627–639, Sep. 2010.



Pinhas Ben-Tzvi (S'02–M'08–SM'12) received the B.S. degree (*summa cum laude*) in mechanical engineering from the Technion—Israel Institute of Technology, Haifa, Israel, in 2000, and the M.S. and Ph.D. degrees in mechanical engineering from the University of Toronto, Toronto, ON, Canada, in 2004 and 2008, respectively.

He is currently an Associate Professor of Mechanical and Aerospace Engineering and the founding Director of the Robotics and Mechatronics Laboratory at The George Washington University, Washington, DC, USA. Before joining the University of Toronto in 2002, he was an R&D Engineer with General Electric Medical Systems Company, developing medical diagnostic robotic and mechatronic systems. His current research interests include robotics and autonomous systems, mechatronics, dynamic systems and control, mechanism/machine design and system integration, and sensing and actuation. Applications include robust dynamic stabilization and agile maneuvering of mobile robots using intelligent biomimetic robotic tails; autonomous

mobile robot mobility and manipulation and modular and reconfigurable mobile robotics for search and rescue, environment monitoring, and defense; advanced devices and robotic systems for medicine; haptics devices and exoskeletons for robot control and rehabilitation; and novel sensors and actuators for biomedical applications. He has authored and co-authored more than 70 peer-reviewed journal articles and refereed papers in conference proceedings and is the inventor of five U.S. patents and a Canadian patent.

Dr. Ben-Tzvi is the recipient of the 2013 GW SEAS Outstanding Young Researcher Award and the GW SEAS Outstanding Young Teacher Award, as well as several other honors and awards. He is a member of the American Society of Mechanical Engineers (ASME).



Zhou Ma (S'10) received the M.S. degree in electrical engineering from the University of Science and Technology, Beijing, China, in 2009, with a thesis focused on kid size humanoid robot. He is currently working toward the Ph.D. degree in the Robotics and Mechatronics Laboratory, Department of Mechanical and Aerospace Engineering, The George Washington University, Washington, DC, USA.

His current research interests include basic and applied research in robotics and mechatronics, and involve investigations in haptics glove design, simulation and optimization, with applications of teleoperation, virtual reality and rehabilitation.